Surface Chemistry

International Edition: DOI: 10.1002/anie.201601037
German Edition: DOI: 10.1002/ange.201601037

Salt-Driven Deposition of Thermoresponsive Polymer-Coated Metal Nanoparticles on Solid Substrates

Zhiyue Zhang, Samarendra Maji, André B. da Fonseca Antunes, Riet De Rycke, Richard Hoogenboom, and Bruno G. De Geest**

Abstract: *Here we report on a simple, generally applicable method for depositing metal nanoparticles on a wide variety of solid surfaces under all aqueous conditions. Noble-metal nanoparticles obtained by citrate reduction followed by coating with thermoresponsive polymers spontaneously form a monolayer-like structure on a wide variety of substrates in presence of sodium chloride whereas this phenomenon does not occur in salt-free medium. Interestingly, this phenomenon occurs below the cloud point temperature of the polymers and we hypothesize that salt ion-induced screening of electrostatic charges on the nanoparticle surface entropically favors hydrophobic association between the polymer-coated nanoparticles and a hydrophobic substrate.*

Nanoparticles and nanostructured films have attracted major interest for a wide variety of applications, including for example biotechnology,[1–3] medicine,[4] photonics,[5–8] microelectronics,[9] and catalysis.[10] In contrast to bulk materials, for which the physicochemical properties are size-independent, many nanoparticle properties strongly depend on particle size and shape.[11,12] Combining bulk materials with a thin coating of a specific nanomaterial therefore allows to engineer the bulk material with unique high added-value properties through the coating.[13] The currently available toolbox for surface modification of solid materials comprises solvent casting,[14] chemical vapor deposition[15] and a wide variety of self-assembly approaches such as Langmuir–Blodgett,[16] layer-by-layer self-assembly,[17–20] and self-assembled monolayer formation.[21,22] In recent years, nature-inspired compounds such as polyphenols and mussel-derived polydopamine that spontaneously deposit on solid substrates have fueled the interest for simple and straightforward surface coating techniques under all aqueous conditions.[23–26] Whereas these methods provide access to all-organic films, there remains an unmet need for simple assembly methods for inorganic nanoparticle coatings under aqueous conditions.

Here we report on a simple, broadly applicable method for depositing metal-nanoparticle films on a wide variety of solid surfaces under all aqueous conditions. Our approach is demonstrated for gold (Au^{NP}) and silver (Ag^{NP}) nanoparticles and allows for extremely easy engineering of bulk materials with plasmonic and catalytic functionality.

Au^{NP} were synthesized by direct reduction of $HAuCl_4$ in aqueous medium in presence of sodium citrate, which acts both as reducing and stabilizing agent.[27,28] Subsequently, the nanoparticles were coated by ligand exchange with defined trithiocarbonate end-functionalized poly(*N*-isopropylacrylamide) (polyNIPAm; PN-3, Table S1 in the Supporting Information; M_n: 4.9 kDa, D: 1.08; Figure 1 A), yielding polyNIPAm@Au^{NP}.[29] PolyNIPAm is a thermoresponsive polymer that undergoes an entropy driven coil-to-globule transition upon heating in aqueous solution with a cloud point temperature (T_{cp}) around 32 °C. Synthesis of this polymer by RAFT (reversible addition–fragmentation chain transfer) polymerization[30] provides direct access to polymers with sulfur-containing end-groups that can form a quasi-covalent bond with metallic gold and silver.[31] Earlier we reported that in water citrate-stabilized polyNIPMAm@Au^{NP} only exhibit reversible temperature-triggered aggregation in presence of NaCl.[29] This behavior was attributed to interparticle electrostatic repulsion by remaining citrate ions on the Au^{NP} surface that is then alleviated upon charge-screening by salt counter ions. Physicochemical properties of the polyNIPAm@Au^{NP} are listed in Table S2 in the Supporting Information and the presence of the polymer coating was also evidenced by TEM (Figure 1 B).

We observed that irrespective of the temperature of the aqueous medium, addition of sodium chloride (NaCl) to an aqueous polyNIPAm@Au^{NP} solution, triggered the deposition of a colored film on the walls of the recipient. Moreover, we also observed that solid substrates that were immersed into solutions that contained 0.1 M NaCl and polyNIPAm@Au^{NP} also became stained. Figure 1 C shows photographs of plastic cuvettes as well as polymethylmethacrylate (PMMA) and glass slides that were coated in this way. Interestingly, control experiments with polyNIPAm@Au^{NP} in absence of salt- or citrate-stabilized Au^{NP} in presence or absence salt do not lead to nanoparticle deposition which clearly indicates the importance of both the thermoresponsive polymer coating as well as the presence of salt (Figure 1 C). Importantly, these deposited polyNIPAm@Au^{NP} films remain fully stable upon repeated washing with water and organic solvents, demonstrating that robust stable nanoparticle coatings are obtained that can be

[*] Z. Zhang, Dr. A. B. da Fonseca Antunes, Prof. B. G. De Geest
Department of Pharmaceutics, Ghent University
Ottergemsesteenweg 460, 9000 Ghent (Belgium)
E-mail: br.degeest@ugent.be
Dr. S. Maji, Prof. R. Hoogenboom
Department of Organic and Macromolecular Chemistry
Ghent University, Krijgslaan 281 S4-bis, 9000 Ghent (Belgium)
E-mail: Richard.hoogenboom@ugent.be
R. De Rycke
Inflammation Research Centre, VIB, Ghent
and
Department of Biomedical Molecular Biology, Ghent University, 9052 Gent (Belgium)

Supporting information for this article can be found under: http://dx.doi.org/10.1002/anie.201601037.

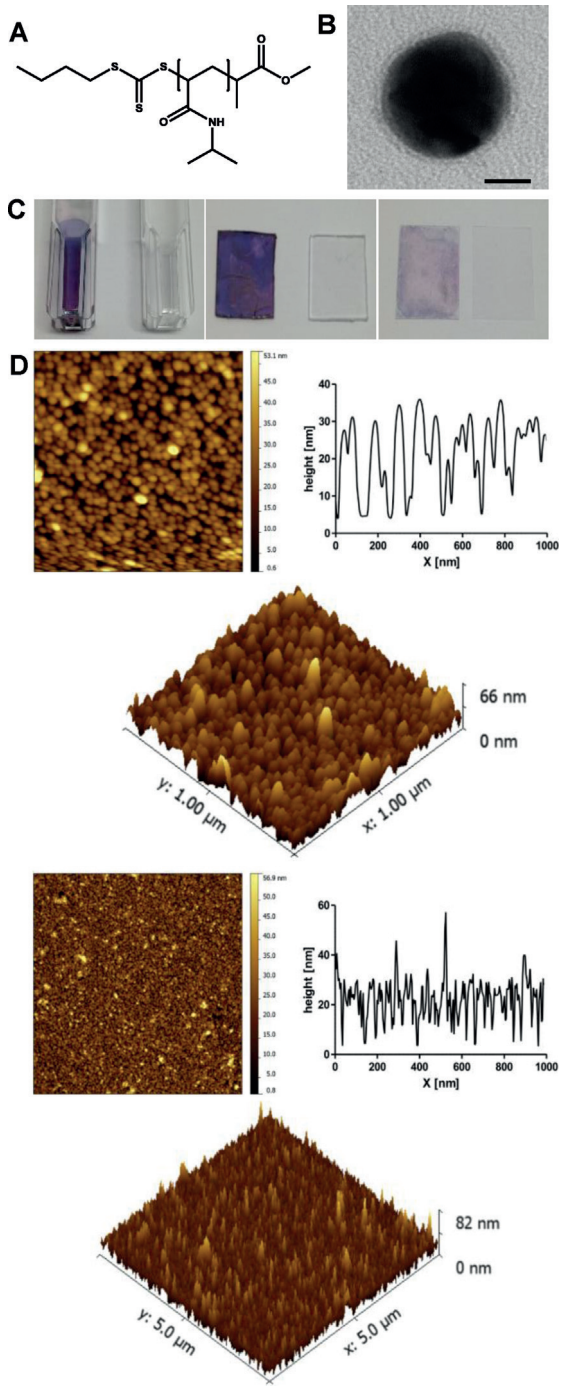

Figure 1. Characterization of polyNIPAm@Au^{NP} and deposited polyNIPAm@Au^{NP} films. A) Molecular structure of polyNIPAm synthesized by RAFT polymerization. B) TEM image of polyNIPAm@Au^{NP}. Scale bar represents 10 nm. C) Photographs of plastic cuvettes, polymethylmethacrylate and glass slides immersed in a polyNIPAm@Au^{NP} solution in the presence (left) or absence (right) of 0.1 M NaCl followed by extensive washing with deionized water. D) AFM images of polyNIPAm@Au^{NP} deposited on silicon wafers.

used for further applications. Atomic force microscopy (AFM) analysis revealed that the deposited film is composed of densely packed polyNIPAm@Au^{NP} that appear to form quasi monolayer-like structure (Figure 1 D). Scanning electron microscopy (SEM) imaging further indicates the coating to consist of a single nanoparticle layer (Figure S2) at an average nanoparticle density of 4700 ± 180 ($n = 2$) nanoparticles per µm^2. Besides Au^{NP}, also Ag^{NP} synthesized by sodium citrate reduction of $AgNO_3$ followed by partial ligand exchange with polyNIPAm, exhibited similar monolayer-forming properties (Figures S1 and S3). Such polyNIPAm@Ag^{NP} coatings could find applications for engineering anti-microbial properties onto a wide variety of substrates, including surgical rubber gloves (see panel b3 in Figure S3).

To investigate whether our findings are unique for polyNIPAm-based systems, we also coated Au^{NP} with other polar polymers that exhibit temperature-responsive behavior (i.e. poly(methoxydiethyleneglycol acrylate) (polyDEGA; $T_{cp} \approx 25\,°C$) and poly(*n*-propyl-2-oxazoline) (poly^{n}PropOx; $T_{cp} \approx 25\,°C$);[32] Figure S4; note that both polymers exhibit hysteresis in turbidimetry measurements; Figure S5) and polar polymers that are fully water-soluble over a broad temperature range (i.e. poly(*N*-vinylpyrrolidone); polyNVP). Interestingly, only the temperature-responsive polymers polyDEGA and poly^{n}PropOx yielded, in presence of 0.1 M NaCl salt, nanoparticle film coatings, whereas in absence of salt no nanoparticle deposition was observed. In case of polyNVP@Au^{NP}, no nanoparticle deposition is observed both in presence or absence of salt, independent of temperature (Figure S4). The unsuccessful deposition of polyNVP@AuNP hints to a hydrophobic driving force for the deposition process as the thermoresponsive polymers have more hydrophobic character. Note that simple casting of polyNIPAm@Au^{NP} from organic solution (i.e. tetrahydrofuran, THF) and subsequent drying and polyNIPAm@Au^{NP} (Figure S6) yields films with a lower coverage and uniformity than films deposited from aqueous NaCl solution. Moreover, whereas deposition by casting and drying from organic solution is possible onto planar substrates, it is not the case for more complex substrates that can easily be coated by spontaneous deposition from aqueous salt solution.

To gain further insights into the driving forces for this salt-induced NP deposition process, we investigated the parameters that play a role in polyNIPAm@Au^{NP} adsorption process. Plastic cuvettes were immersed into solutions of polyNIPAm coated Au^{NP} containing 0.1 M NaCl and the effect on the nanoparticle deposition process of Au^{NP} concentration, deposition time, molecular weight of the polyNIPAm and deposition temperature was studied by UV/Vis spectrophotometry. Because of the surface plasmon resonance (SPR) band of the Au^{NP},[33] UV/Vis spectroscopy is well-suited to measure deposition of the nanoparticles as the absorption intensity provides a measure for the amount of deposition while the maximum absorption wavelength provides information on the proximity of the respective Au^{NP}.[34] Upon deposition of the polyNIPAm@Au^{NP} on the surface of the cuvettes, a shift in the absorption maximum of the SPR band from 526 nm to 584 nm is observed (Figure S7) indicating that the Au^{NP} are found in a more closely aggregated state (i.e. proximity effect) on the cuvette surface, which attributes to the hypothesis that hydrophobic interactions are the driving force for nanoparticle deposition.

As shown in Figure 2 A, nanoparticle deposition increases, as function of the nanoparticle concentration until a plateau is

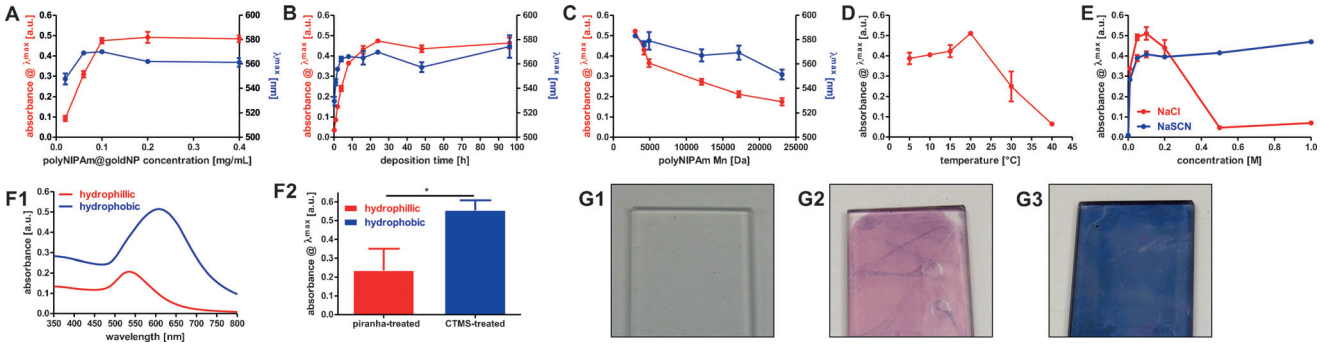

Figure 2. Influence of parameters on polyNIPAm@Au^{NP} deposition. Influence of the A) concentration of polyNIPAm@Au^{NP}, B) deposition time, C) number average molecular weight (M_n) of polyNIPAm, D) deposition temperature, E) salt type and concentration, and F) substrate properties on nanoparticle deposition (red data points) and the plasmon peak (I^{max}; blue data points in panels A–C) of the deposited nanoparticle film, measured by UV/Vis spectrophorometry. (*: $p < 0.05$) All experiments were run in triplicate. Data shown in panels (A–E) were recorded on plastic cuvettes, the data shown in panel (F) was recorded on quartz slides. G) Photographs of quartz slides: (G1) untreated, (G2) treated with piranha and polyNIPAm@Au^{NP}, (G3) treated with piranha, chlorotrimethylsilane (CTMS) and polyNIPAm@Au^{NP}. Unless specifically noted in the respective panels, the conditions for nanoparticle deposition were: polyNIPAm@Au^{NP} concentration of 0.1 mg mL^{-1}, 1 h deposition time, polyNIPAm Mn of 4.9 kDa, 0.1 M NaCl, 20 °C deposition temperature.

reached at a concentration of 0.1 mg mL^{-1} and upwards. A similar trend is observed for the influence of the deposition time (at a fixed nanoparticle concentration of 0.1 mg mL^{-1}), where the amount of adsorbed material increases as function of incubation time until a plateau is reached at 30 min of incubation (Figure 2B). In both cases the plateau has a very similar absorption value of 0.5, which in combination with the smooth surfaces that were observed with AFM and SEM further supports that a monolayer of polyNIPAm@Au^{NP} is deposited. The similar trend observed for the plasmon peak of the deposited film in Figure 2A,B, suggests that increased nanoparticle deposition is accompanied with the nanoparticles being more densely packed. The molecular weight of the polyNIPAm negatively influences the amount of deposited material with a higher molecular weight leading to less adsorbed nanoparticles (Figure 2C). This is again in agreement with the formation of a monolayer of nanoparticles as the larger polymer coatings will decrease the maximum number of deposited nanoparticles per monolayer and is confirmed by the decrease in plasmon peak of the nanoparticle film that can be attributed to the lower packing density of the nanoparticle film. Note that very short polyNIPAm chains (e.g. 1.8 kDa—Figure S8) are incapable of conferring colloidal stability to the polyNIPAm@goldNP in 0.1 M aqueous NaCl solution. When varying the deposition temperature (Figure 2D), nanoparticle deposition does not significantly alters below the T_{cp} of the polyNIPAm, but strongly decreases above the T_{cp}. The latter can be attributed to macroscopic precipitation of the polyNIPAm@Au^{NP} in 0.1 M NaCl at a temperature above the T_{cp} of polyNIPAm as previously reported.[29] The NaCl concentration was found to increase nanoparticle deposition up to a maximum value of 0.1 M whereas higher salt concentrations prevent nanoparticle deposition (Figure 2E). The latter is again due to macroscopic precipitation of polyNIPAm@Au^{NP} from solution at higher salt concentrations. When changing the type of salt from the kosmotropic NaCl to the chaotropic sodium thiocyanate (NaSCN), a slight decrease in nanoparticle deposition occurs up to a salt concentration of 0.1 M. Interestingly, whereas the kosmotrope NaCl induces nanoparticle aggregation in solution above the T_{cp} of the polymer coating, preventing nanoparticle deposition, the chaotrope NaSCN alleviates the temperature-induced aggregation of the nanoparticles, suggesting that its salting in effect renders the polymer coating less hydrophobic. This lower nanoparticle hydrophobicity could explain the slightly lower extent of nanoparticle deposition in presence of NaSCN relative to NaCl. Importantly, both salts induce nanoparticle deposition indicating that the deposition is not driven by the salting in or salting out of the polymer chains. Also note that these salts barely affect the T_{cp} values of polyNIPAm (Figure S9). As such, the deposition process must be related to the charge screening effect, that is, suppression of the electrostatic colloidal stabilization. To investigate the influence of the substrate hydrophobicity we used quartz slides instead of plastic cuvettes. The quartz slides were treated with piranha solution to render them more hydrophilic or treated with piranha plus chlorotrimethylsilane (CTMS) to render them more hydrophobic. As depicted in Figure 2F,G, the nanoparticle deposition is not only more efficient on more hydrophobic surfaces, but also a pronounced blue shift of the SPR band is observed. The latter indicates that CTMS treated quartz slides provide a more hydrophobic environment to the nanoparticles, which favors them to assemble in closer proximity to each other.

Based on these findings, we postulate a hypothesis for the spontaneous deposition of the polymer-coated nanoparticles in presence of salt. The polyNIPAm@Au^{NP} have colloidal stability due to both steric repulsion caused by the polymer chains and electrostatic repulsion. When both are suppressed by heating above the T_{cp} of the polymer and addition of salt, nanoparticle agglomeration occurs in solution. However, below T_{cp} in presence of salt the surface charges are screened while the steric stabilization remains, suppressing interparticle interactions. The polyNIPAm@Au^{NP} in presence of salt are, thus, stabilized by polyNIPAm-water interactions that

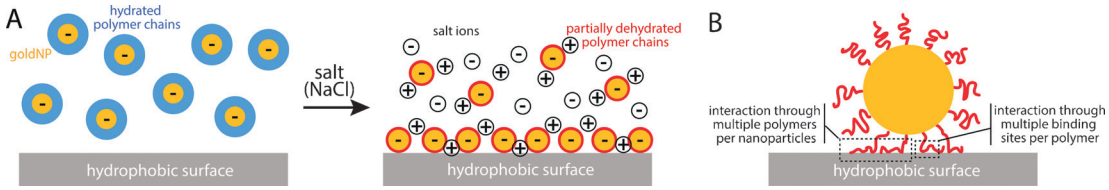

Figure 3. Proposed mechanism for salt-induced deposition of polymer@Au^{NP} on solid surfaces. A) At low ionic strength, polyNIPAm@Au^{NP} remain stable in solution, owing to electrostatic repulsion between the nanoparticles residing from residual citrate anions on the metal nanoparticle surface. At higher ionic strength, the repulsive electrostatic charges are screened and the polymer chains are partially dehydrated because of the salting out effect. This increase in hydrophobicity causes an irreversible adsorption to a more hydrophobic surface. B) Multiple monomeric repeating units per polymer chain and multiple polymer chains per nanoparticle adsorb to the underlying hydrophobic surface accompanied by further polymer dehydration, thereby attributing to the irreversible nature of the nanoparticle deposition.

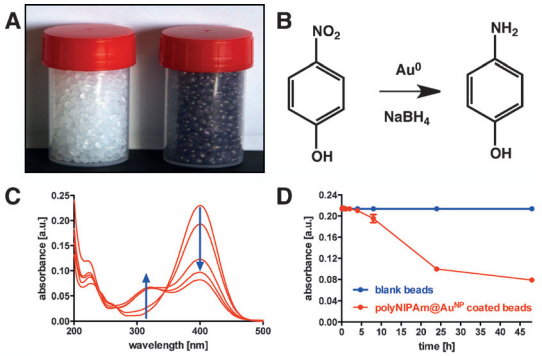

Figure 4. Catalytic activity of the polyNIPAm@Au^{NP} coating. A) Photograph of poly(ethylene-*co*-vinylacetate) beads before (left) and after (right) coating with polyNIPAm@Au^{NP}. B) Reaction Scheme for the conversion of 4-nitrophenol to 4-aminophenol. C) Change in UV/Vis spectrum of the reaction solution catalyzed by polyNIPAm@Au^{NP} coated beads. D) Conversion of 4-nitrophenol to 4-aminophenol as function of time, monitored by UV/Vis absorbance at 400 nm. Experiments were run in triplicate.

compete with polymer-polymer interactions. In presence of a hydrophobic substrate, the hydrophobic polyNIPAm-surface interactions come into play and these hydrophobic interactions in combination with the entropic gain of releasing the hydrating water-molecules is postulated to be the driven force for the polyNIPAm@Au^{NP} deposition process.[35] This process is irreversible because multiple monomeric repeating units per polymer chain and multiple polymer chains adsorb on the surface[13] in combination with polymer dehydration as schematically illustrated in Figure 3B. This proposed mechanism is in good agreement with our experimental observations that the more hydrophilic polyNVP@Au^{NP} do not show deposition and that deposition of polyNIPAm@Au^{NP} is more efficient on more hydrophobic surfaces.

Besides engineering a surface with plasmonic properties owing to the plasmon peak of the Au^{NP}, we aimed as a proof-of-concept at elucidating whether the adsorbed Au^{NP} coating could render a substrate catalytically active. For this purpose, we took poly(ethylene-*co*-vinylacetate) granular beads and immersed these into a 0.1M NaCl solution of polyNIPAm@Au^{NP}. As shown in Figure 4A, the beads gained a pronounced purple colour, indicating successful deposition of a nanoparticle coating. Calculation of the deposited amount of polyNIPAm@Au^{NP} yielded an amount of 0.1 mg of gold per gram of beads (see the Supporting Information). Subsequently, these beads were packed into a column and percolated with a solution of 4-nitrophenol. Metallic gold is able to catalyse the conversion of 4-nitrophenol to 4-aminophenol in presence of sodium borohydride ($NaBH_4$) (Figure 4B), which can be monitored spectrophotometrically by a decrease of the absorption at 400 nm (Figure 4C). Samples were collected after different residence time in the column and the conversion is plotted as function of time (Figure 4D). These data show that, when adsorbed onto the bead surface, the Au^{NP} are still capable of catalyzing a chemical reaction. Control experiments with bare, uncoated, plastic beads did not show any conversion of 4-nitrophenol in presence of $NaBH_4$.

In summary, we have demonstrated that metal nanoparticles coated with a temperature-responsive polymer can undergo salt-induced adsorption onto solid substrates. We attribute this behaviour mainly to hydrophobic interaction between the metal surface and the substrate, which is facilitated by screening residual charges on the metal nanoparticle surface by addition of salt ions. Furthermore, we provide a proof-of-concept that this method allows engineering surfaces with specific functionalities attributed to the presence of the adsorbed nanoparticles. We foresee this approach to be broader applicable to different kinds of inorganic or organic nanoparticles, with specific functions. Moreover, our approach is not limited to planar substrates only, but is capable of coating substrates with a complex morphology as demonstrated by coating of a rubber glove and poly(ethylene-co-vinylacetate) beads.

Experimental Section

Experimental details and additional experimental data can be found the Supporting Information section.

Acknowledgements

Z.Z. acknowledges the Chinese Scholarship council (CSC) for funding. S.M., BGDG and R.H. acknowledges the FWO Flanders and Ghent University (BOF) for funding. Victor de la Rosa is acknowledged for experimental help.

Keywords: gold nanoparticles · polymers · self-assembly · surface chemistry · thin films

How to cite: *Angew. Chem. Int. Ed.* **2016**, *55*, 7086–7090
Angew. Chem. **2016**, *128*, 7202–7206

[1] G. M. Whitesides, *Nat. Biotechnol.* **2003**, *21*, 1161–1165.
[2] P. A. Guerette, et al., *Nat. Biotechnol.* **2013**, *31*, 908–915.
[3] P. D. Howes, R. Chandrawati, M. M. Stevens, *Science* **2014**, *346*, 53–63.
[4] E. K.-H. Chow, E. Pierstorff, G. Cheng, D. Ho, *ACS Nano* **2008**, *2*, 33–40.
[5] M. Ibn-Elhaj, M. Schadt, *Nature* **2001**, *410*, 796–799.
[6] S. Lal, S. Link, N. J. Halas, *Nat. Photonics* **2007**, *1*, 641–648.
[7] J. Hiller, J. D. Mendelsohn, M. F. Rubner, *Nat. Mater.* **2002**, *1*, 59–63.
[8] P. Long, et al., *Adv. Mater.* **2013**, *25*, 5621–5625.
[9] G. Eda, G. Fanchini, M. Chhowalla, *Nat. Nanotechnol.* **2008**, *3*, 270–274.
[10] K. Kishimoto, et al., *J. Am. Chem. Soc.* **2005**, *127*, 15618–15623.
[11] R. C. Jin, et al., *Nature* **2003**, *425*, 487–490.
[12] R. C. Jin, et al., *Science* **2001**, *294*, 1901–1903.
[13] S. Rose, et al., *Nature* **2014**, *505*, 382–385.
[14] H. Y. Erbil, A. L. Demirel, Y. Avci, O. Mert, *Science* **2003**, *299*, 1377–1380.
[15] A. Reina, et al., *Nano Lett.* **2009**, *9*, 30–35.
[16] J. A. Zasadzinski, R. Viswanathan, L. Madsen, J. Garnaes, D. K. Schwartz, *Science* **1994**, *263*, 1726–1733.
[17] N. A. Kotov, I. Dekany, J. H. Fendler, *J. Phys. Chem.* **1995**, *99*, 13065–13069.
[18] G. Decher, *Science* **1997**, *277*, 1232–1237.
[19] Y. Kim, et al., *Nature* **2013**, *500*, 59–63.
[20] D. Lee, M. F. Rubner, R. E. Cohen, *Nano Lett.* **2006**, *6*, 2305–2312.
[21] A. K. Boal, et al., *Nature* **2000**, *404*, 746–748.
[22] D. Y. Ryu, K. Shin, E. Drockenmuller, C. J. Hawker, T. P. Russell, *Science* **2005**, *308*, 236–239.
[23] H. Lee, S. M. Dellatore, W. M. Miller, P. B. Messersmith, *Science* **2007**, *318*, 426–430.
[24] Q. Wei, et al., *Angew. Chem. Int. Ed.* **2014**, *53*, 11650–11655; *Angew. Chem.* **2014**, *126*, 11834–11840.
[25] H. Ejima, et al., *Science* **2013**, *341*, 154–157.
[26] T. S. Sileika, D. G. Barrett, R. Zhang, K. H. A. Lau, P. B. Messersmith, *Angew. Chem. Int. Ed.* **2013**, *52*, 10766–10770; *Angew. Chem.* **2013**, *125*, 10966–10970.
[27] J. Turkevich, P. C. Stevenson, J. Hillier, *Faraday Soc.* **1951**, *11*, 55–75.
[28] G. Frens, *Nat. Phys. Sci.* **1973**, *241*, 20–22.
[29] Z. Zhang, et al., *Chem. Mater.* **2013**, *25*, 4297–4303.
[30] G. Moad, E. Rizzardo, S. H. Thang, *Aust. J. Chem.* **2005**, *58*, 379–410.
[31] B. S. Sumerlin, et al., *Langmuir* **2003**, *19*, 5559–5562.
[32] V. R. de la Rosa, Z. Y. Zhang, B. G. De Geest, R. Hoogenboom, *Adv. Funct. Mater.* **2015**, *25*, 2511–2519.
[33] L. M. Liz-Marzán, C. J. Murphy, J. F. Wang, *Chem. Soc. Rev.* **2014**, *43*, 3820–3822.
[34] T. Pradeep, B. R. Buergi, A. Chainani, J. Chakrebarti, S. K. Das, N. DasGupta, P. A. Joy, M. A. H. Muhammed, etc. *A Textbook of Nanoscience and Nanotechnology*, Tata McGraw Hill Education Private Limited, New Delhi, **2012**.
[35] M. A. Plunkett, Z. H. Wang, M. W. Rutland, D. Johannsmann, *Langmuir* **2003**, *19*, 6837–6844.

Received: January 29, 2016
Revised: March 10, 2016
Published online: May 3, 2016

